Eur. Phys. J. B **5**, 79–85 (1998)

THE EUROPEAN PHYSICAL JOURNAL B

Strong anisotropic nematic order in liquid crystal polymers: a quasi-elastic neutron scattering study

S. Lecommandoux[1], F. Hardouin[1] and A.J. Dianoux[2,a]

[1] Centre de Recherche Paul Pascal, avenue A. Schweitzer, 33600 Pessac, France
[2] Institut Laue Langevin, 156X, 38042 Grenoble Cedex, France

Received: 29 October 1997 / Revised: 22 January 1998/ Accepted: 11 May 1998

Abstract. From quasi-elastic neutron scattering experiments performed in glassy, nematic and isotropic phases, the dynamics of oriented samples of strong anisotropic side-on fixed liquid crystal polymers have been analysed. Using the selective deuteration method, we are able to attribute motions to specific parts of the molecule in the parallel and perpendicular orientations. The motions of the whole macromolecule decrease as soon as the temperature decreases below the isotropic-nematic transition. Nevertheless, the motions of the polymer backbone, compared to the whole polymer dynamics, are systematically reduced, even in the isotropic phase. Moreover, an anisotropy of the motions is revealed, with a reduction in the direction parallel to the orientation. An harmonic character of the vibrational processes is also evidenced. We conclude that the anisotropy of the dynamic corroborates the anisotropy of conformation of the macromolecule (so-called jacketed structure).

PACS. 61.30.-v Liquid crystals – 62.20.-x Mechanical properties of solids – 66.20.+d Viscosity of liquids; diffusive momentum transport

1 Introduction

Tremendous efforts have been made to synthesise liquid Crystal polymers (LCPs) in the last decades and many experiments have been performed to investigate the dependence of the polymeric and mesomorphic properties upon their molecular architecture. In LCPs, the tendency of the polymer chains to maximise their entropy is counterbalanced by orientational ordering effects resulting from anisotropic interactions between mesogenic units. Such antagonism occupies a central position in polymer physics.

In the last years, we had specifically studied the shape and sizes of the polymer backbone for "side-on fixed" LCPs. In these compounds, the mesogenic groups are laterally attached to the backbone *via* more or less flexible spacer, in opposition with "side-end fixed" LCPs which form another class of side chain LCPs (Fig. 1).

In the "side-on" family, the nematic state is usually favoured for short spacers (named n) and short aliphatic tails (named m). More recently, we have shown that it was possible to obtain a nematic to smectic C polymorphism in this kind of systems [1]. Backbone conformation studies on these LCPs by small angle neutron scattering has revealed, for short spacer n and short aliphatic tails m, that the polymer chain is strongly stretched, on average, in the direction imposed by the mesogenic groups laterally attached. A tentative representation is a strong jacketed nematic structure [2,3] illustrating at the scale of the chain dimension the favourable geometric coupling between the chain and the mesogenic units. Moreover, we have recently described the chain conformation of this LCP with a model of homogeneous and well-oriented cylinders [4]. The experimental data well fitted by this model result in a polymer conformation in the nematic phase which is totally extended like a rod without hairpin defect [5].

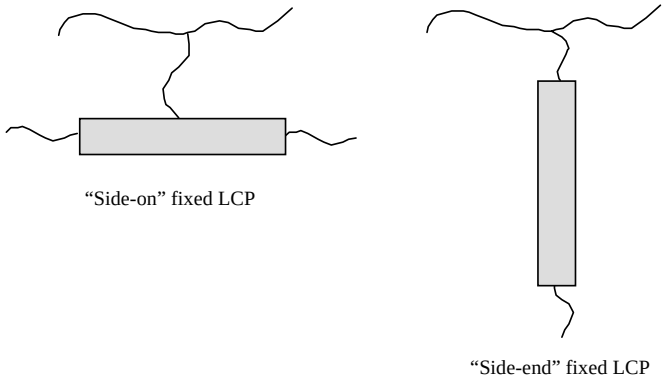

Fig. 1. Schematic representation of a "side-on" and "side-end" fixed liquid crystal polymer.

In this paper, we aim at studying such a jacketed LCP in order to answer this question: is the anisotropy of the shape of the backbone correlated to an anisotropy of the motions of the macromolecule?

[a] e-mail: dianoux@ill.fr

2 Theory [6,7]

The dynamical studies have been performed by quasi-elastic neutron scattering using Time of Flight spectrometers. The scattered intensity is proportional to the incoherent scattering function $S_{inc}(\mathbf{Q},\omega)$:

$$S_{inc}(\mathbf{Q},\omega) = \int_{-\infty}^{+\infty} dt\, e^{-i\omega t} \sum_i (b_i^{inc})^2 \langle e^{i\mathbf{Q}\mathbf{r}_i(0)} e^{-i\mathbf{Q}\mathbf{r}_i(t)} \rangle \quad (1)$$

where b_i^{inc} is the incoherent scattering length of the atom i, $\mathbf{r}_i(0)$ is the position of the atom i at time zero and $\mathbf{r}_i(t)$ is the position of the atom i at time t.

The scattering length b_i^{inc} for hydrogen is bigger than for all other nuclei by more than one order of magnitude: in first approximation, only the motions of protons need to be considered. For uncoupled motions, we can write with obvious notations:

$$\mathbf{r}_i(t) = \mathbf{c}_i(t) + \mathbf{l}_i(t) + \mathbf{u}_i(t) \quad (2)$$

where $\mathbf{c}_i(t)$ is the translational part, $\mathbf{l}_i(t)$ is the rotational part and $\mathbf{u}_i(t)$ is the vibrational part.

In the quasi-elastic region, the vibrational part manifests itself by a Debye-Waller factor $e^{-Q^2\langle u^2\rangle}$, where $\langle u^2\rangle^{1/2}$ is the vibrational amplitude. The scattering law becomes a sum of elementary curves (Lorentzian). We can write:

$$S_{inc}(\mathbf{Q},\omega) = e^{-Q^2\langle u^2\rangle} \left[S_{inc}^R(\mathbf{Q},\omega) \otimes S_{inc}^T(\mathbf{Q},\omega) \right] + B(\mathbf{Q}) \quad (3)$$

where $S_{inc}^R(\mathbf{Q},\omega) \otimes S_{inc}^T(\mathbf{Q},\omega)$ is the convolution product of the rotational part (S_{inc}^R) with the translational part (S_{inc}^T). $B(\mathbf{Q})$ contains the low frequency tail of the vibrational modes. In general, molecules in solid state do not have long range translational motions. We can approximate at each angle the quasi-elastic function as a Lorentzian function $L(\mathbf{Q},\omega)$. This gives the experimental scattering law:

$$S_{inc}(\mathbf{Q},\omega) = e^{-Q^2\langle u^2\rangle} \times \Big[EISF(\mathbf{Q})\delta(\omega) + (1 - EISF(\mathbf{Q}) \times L(\mathbf{Q},\omega) \Big] + B(\mathbf{Q}) \quad (4)$$

where $EISF(\mathbf{Q})$ is the elastic incoherent structure factor which gives informations on the geometry of the motions, an $\delta(\omega)$ is a Dirac function.

In spite of all these possibilities, quasi-elastic neutron scattering experiment is rarely used to study polymers. Since about twenty years, new sources bringing higher resolutions and flux [8], have permitted studies on hydrogen in metals [9], methane in zeolithes [10], liquid crystals [11], polymers [12], liquid crystal polymers [13].

3 System under study and experimental part

We choose to study the side-on fixed LCP with high anisotropic backbone conformation: PA_{444} (polyacrylate) [14]. In order to simplify the interpretation, we work on the completely hydrogenated polymer $PA_{444}H$ or on the partially deuterated one $PA_{444}D$. The chemical formulae is given in Figure 2 and the transition temperatures are given in Table 1.

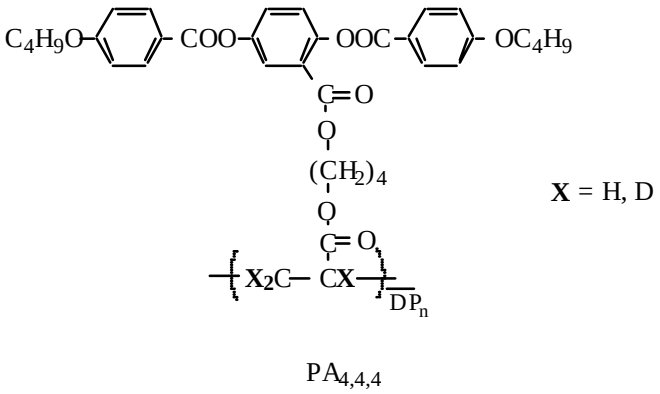

Fig. 2. Chemical formula of the polyacrylate PA_{444} hydrogenated (X = H) and deuterated on the backbone (X = D).

Table 1. Transition temperatures (°C) for the polymers under study. g: glassy state. N: nematic phase. I: isotropic phase.

Polymer	Transition Temperatures (°C)				
	g	•	N	•	I
$PA_{444}H$		40		126	
$PA_{444}D$		39		126	

The selective deuteration allows to neglect some motions and will help the interpretation. Nevertheless, the complexity of the non-deuterated parts (spacer, aliphatic tails, aromatic protons) will be a limitation.

The samples have been beforehand oriented in the cell plane (cell in aluminium AU5, thickness 0.2 mm and 0.5 mm, useful diameter of 3 cm) by decreasing the temperature from the isotropic phase under a magnetic field of 4 T. Thus, experiments are possible in glassy, nematic and isotropic phases.

This study has been performed on the Time of Flight spectrometers IN5 and IN6 at the ILL-Grenoble (France). Different experimental conditions have been chosen in order to use various resolutions (Tab. 2).

Using two different experimental geometries shown in Figure 3 [15], it is possible to differenciate the motions in the direction parallel ($\parallel$) or perpendicular ($\perp$) to the nematic director, that is to the orientation imposed by the magnetic field.

Let's see now the physical parameters we aim at studying in order to better understand our system, and generally all systems of LCP. Experimentally, it is important to separate the elastic contribution and the quasi-elastic part which contains the contribution of all the motions. The elastic part is given by the spectrum of a completely elastic material (vanadium). Then, we can fit the quasi-elastic part with one or several Lorentzians. An example of experimental data and fits is given in Figure 4.

Table 2. Experimental conditions used.

Spectrometer	Incident wavelength λ (Å)	Resolution (μeV)	Transfer of moment Q (Å^{-1})	Characteristic Time τ (s)
IN6	5.12	100	$0.35 \leq Q \leq 1.93$	10^{-11}–10^{-12}
IN5	6	63	$0.29 \leq Q \leq 1.73$	10^{-11}
IN5	10	14	$0.15 \leq Q \leq 1.05$	10^{-10}

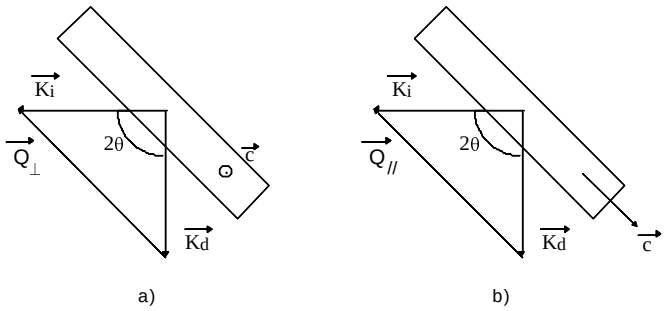

Fig. 3. The different experimental geometries. $\mathbf{K_i}$ is the incident wave vector. $\mathbf{K_d}$ is the scattered wave vector. $\mathbf{Q}$ is the momentum transfer. (a) Perpendicular geometry $C_\perp$: $\mathbf{Q}$ is perpendicular to the orientation of the mesogens. (b) Parallel geometry $C_\parallel$: $\mathbf{Q}$ is parallel to the orientation of the mesogens for $2\theta \approx 90^\circ$.

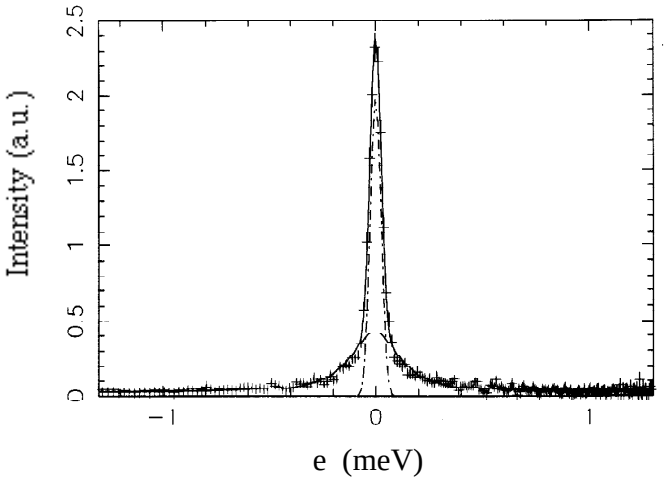

Fig. 4. Exemple of a Time of Flight spectrum for PA_{444} in the nematic phase. (_ _ _) Elastic part, (_ _ _ _) quasi-elastic part, (——) global spectrum.

It is now possible to calculate the EISF (Eq. (4)) which corresponds to the elastic intensity I_e divided by the total intensity (elastic I_e + quasi-elastic I_q):

$$EISF = \frac{I_e}{I_e + I_q} \cdot \tag{5}$$

Moreover, the average width of the Lorentzian calculated for the quasi-elastic contribution gives the correlation time τ of rotational or translational motions (with 1 meV = 1.52×10^{12} rad s^{-1}).

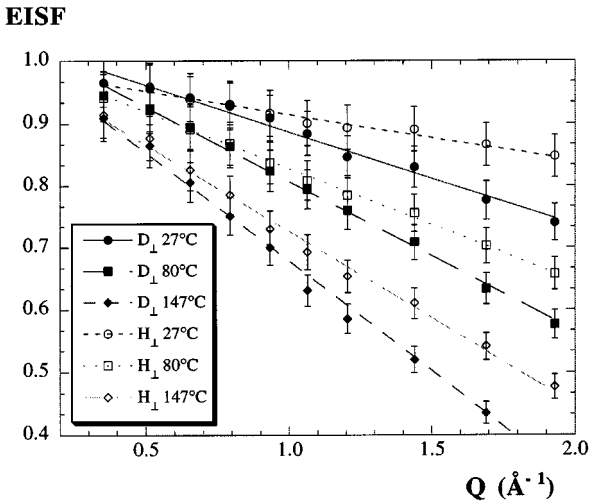

Fig. 5. EISF as a function of $\mathbf{Q}$ for $PA_{444}H$ and D at different temperatures in the direction perpendicular ($\perp$) to the orientation.

Finally, it is possible to deduce the Debye-Waller factor $e^{-2W_1} = e^{-Q^2\langle u^2\rangle}$. This factor comes from very fast vibrational motions of the protons.

4 Experimental results

We have studied the dynamical contributions of our samples in the directions parallel and perpendicular to the orientation of the mesogenic groups, using three resolutions (see Tab. 2).

4.1 Fast motions: low resolution

The spectra obtained (spectrometer IN6 - incident wavelength $\lambda = 5.12$ Å) have been analysed as the superposition of an elastic scattering (fitted with the resolution function) and a quasi-elastic scattering (fitted with a Lorentzian). We have realised this fitting for each angle, each compound and each temperature. The average width of the Lorentzian is around 0.17 meV in the glassy, nematic and isotropic phases. This corresponds to characteristic times τ equal to 4×10^{-12} s. The resultant EISF (Eq. (5)) is represented as a function of Q for the $PA_{444}H$ and D in Figures 5 and 6.

Figure 5 shows first that the EISF is systematically higher for the hydrogenated polymer than for the deuterated one in the direction perpendicular. This shows that

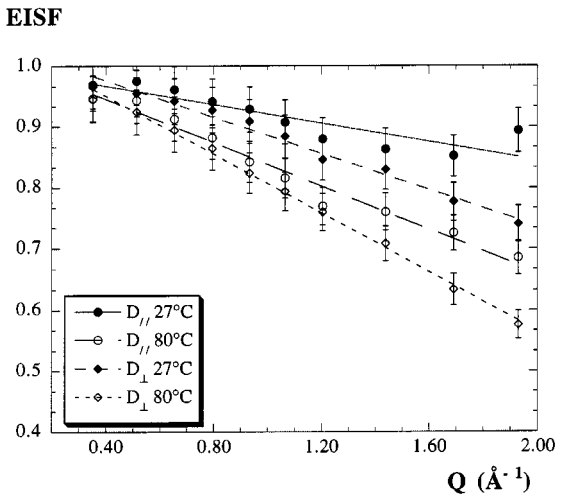

Fig. 6. EISF as a function of **Q** for $PA_{444}D$ at different temperatures in the directions parallel (∥) and perpendicular (⊥) to the orientation.

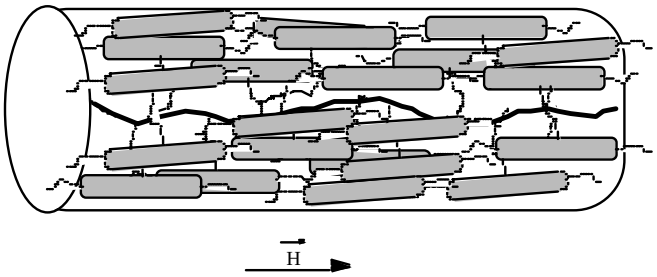

Fig. 7. Schematic representation of the jacketed structure. **H** is the magnetic field imposed.

the observed motions essentially come from the mesogens. Moreover, Figure 6 reveals that the motions are systematically reduced in the direction parallel to the imposed orientation. This can be interpreted as a consequence of the jacketed effect evidenced in this sample [14,15]. In the jacketed model, the polymer backbone is strongly anisotropic and stretched by its mesogenic groups (Fig. 7). A quasi-locking of translational motions in the direction parallel can arise from this jacketed effect.

We also see, that the elastic intensity is high, even in the isotropic state ($T = 147$ °C): this shows the rigidity of the polymer backbone. This corroborates with previous findings by small angle neutron scattering on this system revealing a rod-like behaviour of the backbone [4] in the nematic state.

These informations are more or less given in Figure 8 which represents the EISF as a function of the temperature T for a particular Q value: the increase of the EISF when T decreases can be explained by two facts. Either there is a decrease of the number of protons contributing to the quasi-elastic scattering because the characteristic time of their motions becomes too long, or there is a decrease of the volume swept by the protons. Obviously, these two possibilities can occur together: in the compound studied there are many kinds of protons (polymer backbone, spacer, aliphatic tails, aromatic protons). This figure also shows an EISF lower for the deuterated compound in the perpendicular direction revealing preferential motions of the liquid crystal part in the direction perpendicular to the orientation.

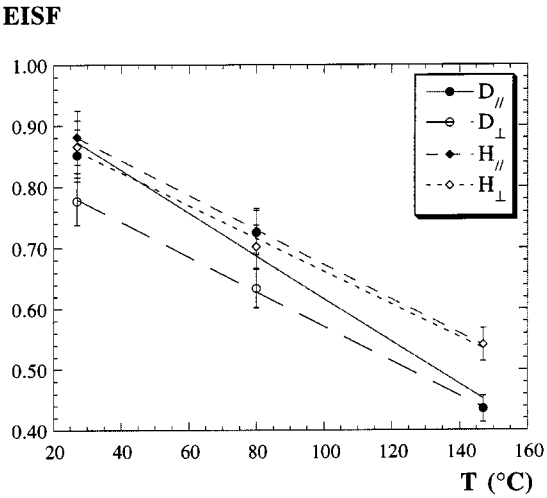

Fig. 8. EISF as a function of temperature for $PA_{444}H$ and D in the directions parallel (∥) and perpendicular (⊥). Resolution 100 μeV. $Q = 1.69$ Å^{-1} ($2\theta \approx 90°$). Lines are just a guide for the eye.

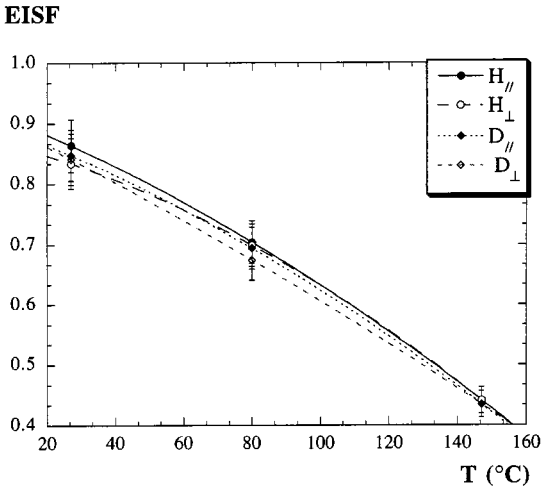

Fig. 9. EISF as a function of temperature for $PA_{444}H$ and D in the directions parallel (∥) and perpendicular (⊥). Resolution 63 μeV. $Q = 1.50$ Å^{-1} ($2\theta \approx 90°$). Lines are just a guide for the eye.

We will now analyse the measurements realised at medium resolution.

4.2 Medium resolution

We have followed the same method of analysis as before to interpret the data obtained on the spectrometer IN5 with a wavelength $\lambda = 6$ Å. The Lorentzian width obtained are the same for each compound (~ 0.1 meV), corresponding

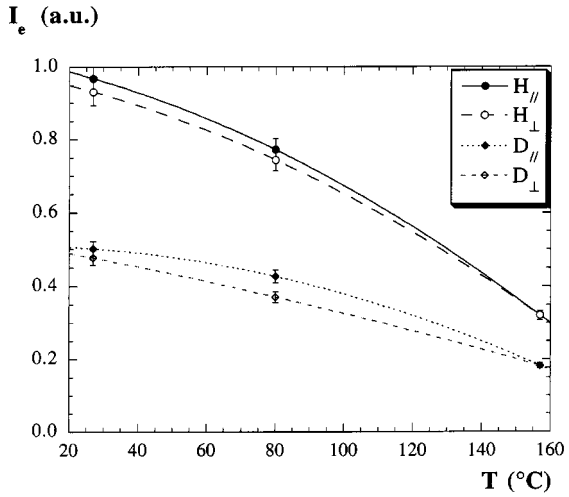

Fig. 10. Scattered elastic intensity I_e as a function of temperature for $PA_{444}H$ and D in the directions parallel ($\|$) and perpendicular ($\perp$). Resolution 14 μeV. $Q = 0.90$ Å^{-1} ($2\theta \approx 90°$). Lines are just a guide for the eye.

to a characteristic time $\tau = 6.6 \times 10^{-12}$ s. The evolution of the EISF for a particular angle as a function of the temperature T is represented in Figure 9 for the PA_{444}. This figure does not show significative differences: we have always the same increase of the EISF when T decreases showing a decrease in the macromolecular motions. At this resolution (63 μeV) we can say that no anisotropy of the polymer backbone is observed, neither in the direction parallel nor in the direction perpendicular to the magnetic field direction. At the characteristic time explored, we see uniform motions of the whole macromolecule.

4.3 High resolution

We will now try to fit the data obtained on the spectrometer IN5 ($\lambda = 10$ Å) with two Lorentzians. For the first one $L1$ (width = 0.1 meV - $\tau_1 = 6.6 \times 10^{-12}$ s), we take the width we found before (resolution 63 μeV) in order to take into account the faster motion. The second one $L2$ (width = 0.01 meV)will fit the rest of the spectrum.

The resolution of 14 μeV reveals a second Lorentzian ($L2$) corresponding to longer characteristic time ($\tau_2 = 6.5 \times 10^{-11}$ s). So we have determined an elastic intensity I_e (resolution function), a quasi-elastic intensity of fast motions I_{q1} and a quasi-elastic intensity of slow motions I_{q2}. Figure 10 shows the evolution of I_e as a function of the temperature T. It appears clearly that the elastic intensity of the hydrogenated polymer is much bigger than the deuterated one. This reveals an important elastic contribution of the backbone (at this high resolution) and a dynamic hindrance in its motions (certainly due to the jacketed effect). Moreover, the intensity I_e is always more important in the direction parallel: a molecular dynamic anisotropy is also observed.

By another way, the fit with two Lorentzians can allow us to characterise rotational or translational motions.

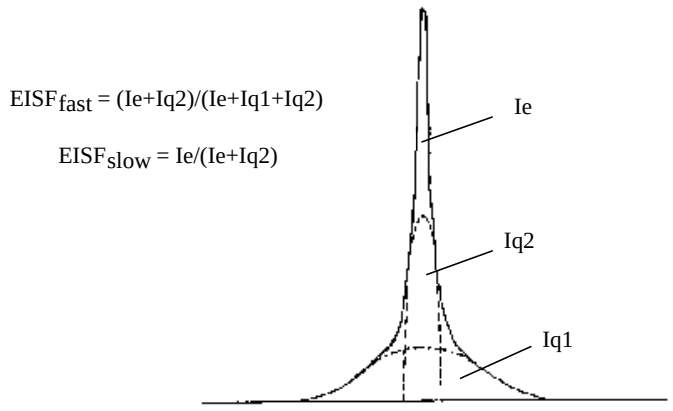

Fig. 11. Schematic representation of the determination of the EISF for slow motions ($EISF_{slow}$) and for fast motions ($EISF_{fast}$).

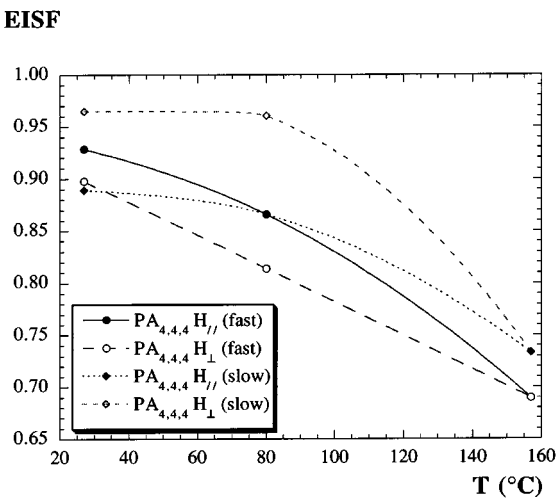

Fig. 12. ($EISF_{slow}$) and ($EISF_{fast}$) as a function of temperature for $PA_{444}H$ in the directions parallel ($\|$) and perpendicular ($\perp$). Resolution 14 μeV. $Q = 0.91$ Å^{-1} ($2\theta \approx 90°$). Lines are just a guide for the eye.

In fact, according to Volino [16], the elementary curve (Lorentzian) with a small width corresponds essentially to the translational contribution. The elementary curve with large width corresponds to a superposition of rotation + translation. The determination of I_{q1} and I_{q2} as represented in Figure 11 allows us to calculate two EISFs: one for the fast motions ($EISF_{fast}$) and one for the slow motions ($EISF_{slow}$).

The evolution of these EISFs as a function of the temperature T is shown in Figures 12 and 13 for the $PA_{444}H$ and $PA_{444}D$ respectively. Figure 12 shows for the $PA_{444}H$ a significative difference of the $EISF_{slow}$ in the two directions ($\|$ and $\perp$): there is more translational motions of the polymer in the parallel direction. The ($EISF_{fast}$) does not reveal such a behaviour. For the $PA_{444}D$ (Fig. 13), slow motions have the same evolution. On the other hand, fast motions are slightly more important in the parallel direction, this seems in contradiction with the results obtained with the other resolutions. Finally, comparing Figures 12

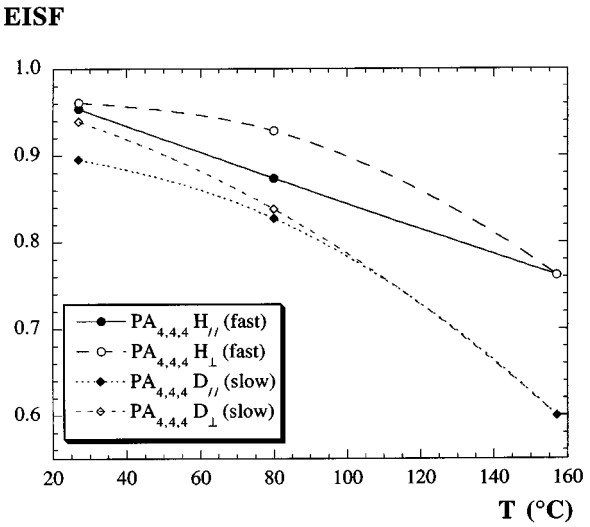

Fig. 13. ($\mathrm{EISF_{slow}}$) and ($\mathrm{EISF_{fast}}$) as a function of temperature for $\mathrm{PA_{444}}$ in the directions parallel ($\|$) and perpendicular ($\perp$). Resolution 14 μeV. $Q = 0.91$ Å^{-1} ($2\theta \approx 90°$). Lines are just a guide for the eye.

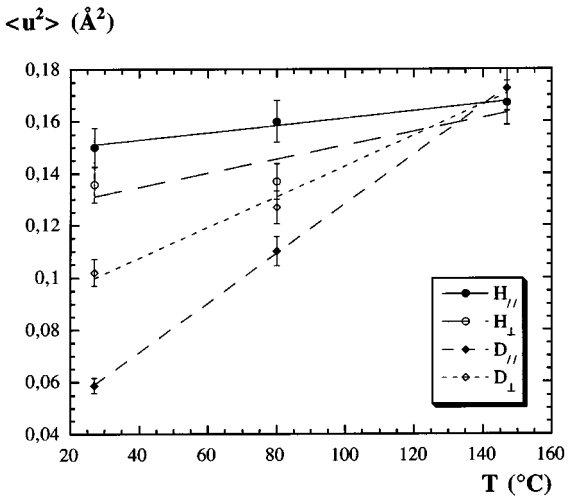

Fig. 14. Evolution of $\langle u^2 \rangle$ as a function of temperature for $\mathrm{PA_{444}H}$ and D in the directions parallel ($\|$) and perpendicular ($\perp$). Resolution 100 μeV.

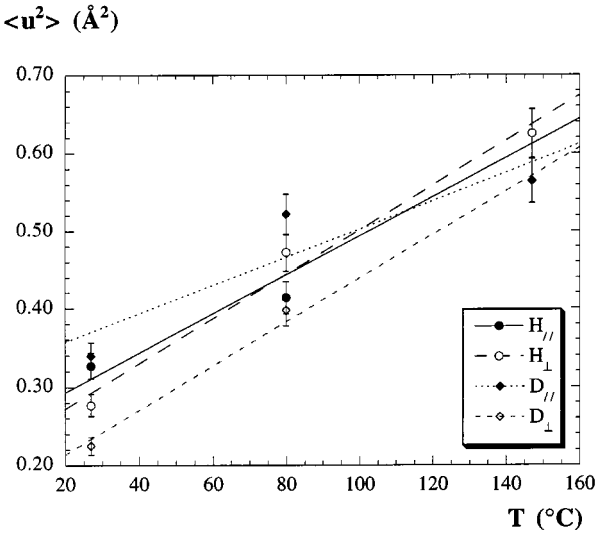

Fig. 15. Evolution of $\langle u^2 \rangle$ as a function of temperature for $\mathrm{PA_{444}H}$ and D in the directions parallel ($\|$) and perpendicular ($\perp$). Resolution 14 μeV.

and 13, we have to note that the values of ($\mathrm{EISF_{slow}}$) stay high, in agreement with the fact that the polymer backbone is confined and constrained.

4.4 Vibrational processes

After the study of the quasi-elastic part, we are interested in the vibrational processes and their evolution as a function of the temperature. In fact, the scattered intensity is a function of the Debye-Waller factor $e^{-Q^2\langle u^2 \rangle}$ (Eq. (4)). The slope of the plot of the logarithm of the total intensity $I_e + I_q$ as a function of Q^2 gives the mean square amplitude of the vibrational motions of the protons $\langle u^2 \rangle$. Thus it is possible to determine $\langle u^2 \rangle$ for each compound, each temperature and each resolution (100 μeV, 63 μeV, 14 μeV).

Figure 14 represents the evolution of $\langle u^2 \rangle$ for $\mathrm{PA_{444}H}$ and D in the orientation parallel and perpendicular as a function of the temperature T (resolution 100 μeV). It reveals first a linear evolution of $\langle u^2 \rangle$ with T which shows the harmonic character of the vibrational processes. Moreover, the amplitude of the fast vibrational motions in the isotropic phase is the same for the hydrogenated and deuterated polymers: all the protons vibrate with the same amplitude $\langle u^2 \rangle^{1/2} = 0.4$ Å. Nevertheless, the temperature evolution for the hydrogenated polymer is smoother than for the deuterated one, with $\langle u^2 \rangle$ systematically bigger. This shows that there is a certain contribution of the backbone protons to the vibrational processes. Thus, comparing with the study of the EISFs, we can say that, even if the motions of the polymer backbone are very small at this resolution, quick vibrations of these protons exist. The same treatment has been realised for the medium and high resolution data (63 μeV and 14 μeV). As we can see on Figure 15 (for the resolution of 14 μeV), no significative differences are noted. We can deduce that the participation of the polymer and the liquid crystal part are about the same. Furthermore, one notes that the amplitude of the vibrational motions is much higher for the slow diffusive motions evidenced with the high resolution experiments.

5 Discussion and conclusion

This paper presents the first dynamical study of a side-on fixed LCP in the isotropic, nematic, and glassy phases using neutron time of flight spectrometry. We have studied various polymers, selectively deuterated or not, and we are able to attribute certain motions, observed in the direction

parallel and perpendicular to the global orientation, to relatively precise parts of the macromolecule.

We have to stress that we are not able to deduce qualitative evolutions without a modelization of all the parameters. Moreover, we do not have any reference on the dynamical properties of these kind of complicated macromolecules, and polymers generally exhibit complex relaxation functions. That is why we have adopted a simple procedure of data evaluation that could appear arbitrary. We could have chosen to fit our data with a stretched exponential, and more precisely to the Fourier transform of a stretched exponential, which is not an analytical function. The stretched exponential relaxation function corresponds to a distribution of relaxation times. We have here taken the hypothesis to consider only two terms in this distribution, and thus only two contributions to the quasielastic part. Moreover, when the elastic to quasielastic separation is clear, as shown in Figure 4, the EISF concept is useful: we may not have been able to fit these data with the Fourier transform of only one stretched exponential but we would have had to add an elastic contribution. To simplify, we have chosen to fit the elastic contribution with the resolution function, and the quasielastic contribution with a Lorentzian. Nevertheless, we have obtained real and important results concerning the dynamical behaviour of such complex and anisotropic systems.

For the mesogenic groups, many motions are observed, even in the glassy state: the polymer part is freezed but rotational, translational and vibrational modes remain in the liquid crystal part. In each phase, a systematic reduction of the mesogenic motions is evidenced in the direction parallel to their orientation.

Concerning the polymer backbone, we have revealed an important participation to the elastic scattering corresponding to an important rigidity, even in the isotropic state. The motions of the backbone are thus strongly reduced compared to the whole macromolecule. Moreover, the restriction of the motions of the backbone is more important in the direction parallel to the nematic orientation.

All these observations corroborate with the jacketed model: locally and globally the polymer backbone is stretched and constrained in the direction of the nematic field imposed by its mesogenic groups. We have a correlation between the anisotropy of conformation of the polymer backbone and the anisotropy of the molecular dynamics observed here. In this sense, we can think that the microscopic interactions of the system can determine the behaviour at the scale of the polymer.

Finally, considering the error bars of the values of $\langle u^2 \rangle$ in the different phases, we are not able to see discontinuities at the phase transitions: in first approximation, we can suppose that the vibrational processes have an harmonic character in the whole temperature range examined. Another novel result is the presence of fast vibrational motions of the protons of the polyacrylate chains with a small amplitude ($\langle u^2 \rangle^{1/2} = 0.5$ Å) in the nematic phase. Even if the motions of the polymer backbone are reduced, small amplitude vibrational modes remained.

Fruitful and stimulating discussion with F. Guillaume are gratefully acknowledged. Furthermore, we thank the RMN group of the Centre de Recherche Paul Pascal for the help in the orientation of the samples.

References

1. M.F. Achard, S. Lecommandoux, F. Hardouin, Liquid Crystals **19**, 581 (1995).
2. Qi-Feng Zhou, Min-Hui Li, Xin-De Feng, Macromol. **20**, 233 (1987).
3. F. Hardouin, S. Méry, M.F. Achard, M. Mauzac, P. Davidson, Liquid Crystals **8**, 565 (1990).
4. S. Lecommandoux, M.F. Achard, F. Hardouin, A. Brûlet, J.P. Cotton, Liquid Crystals **22**, 549 (1997).
5. P.G. De Gennes, *The Physics of Liquid Crystals*, (Oxford Press, U.K, 1974).
6. J.S. Higgins, H.C Benoît, *Polymer and Neutron Scattering*, (Lovesey et Mitchell. Ed., Oxford Science Publications, 1994).
7. M. Bée, *Quasi-Elastic Neutron Scattering*, (Adam Hilger Ed., 1988).
8. F. Volino, A.J. Dianoux, *New developments in neutron scattering for the study of molecular systems: structure and diffusive motions*, Proc. of the Euchem Conf. Organic Liquids: Structures, Dynamics and chemical properties, Elmau, RFA, (J. Wiley Ed., 1978) p. 17-47.
9. T. Springer, *Quasi-elastic scattering for the investigation of diffusive motions*, (Springer Tracts für Physics, 1972).
10. W. Press, *Single particle rotations in molecular crystals*, (Springer Tracts für Physics, 1981).
11. H. Hervet, A.J. Dianoux, R.E. Lechner, F. Volino, J. Phys. **37**, 587 (1976).
12. J.S. Higgins in *Treatise on material science and technology*, **15**, 381, edited by G. Kostorz (Academic Press, 1979).
13. L Benguigui, L. Noirez, R. Kahn, P. Keller, M. Lambert, E. Cohen de Lara, J. Phys. II France **1**, 451 (1991).
14. N. Leroux, P. Keller, M.F. Achard, L. Noirez, F. Hardouin, J. Phys. II France **3**, 1289 (1993).
15. J.L. Sauvajol, D. Djurado, A.J. Dianoux, N. Theophilou, J.E. Fisher, Phys. Rev. B **43**, 14305 (1991).
16. F. Volino, Local Dynamics in polyatomic fluids, Chapter III in *Microscopic Structure and Dynamics of Liquids* Nato Asi series B: Physics, **33**, edited by J. Dupuy, A.J. Dianoux (Plenum Press, 1978).